

Sounds in the Ocean at 1–100 Hz

William S.D. Wilcock,¹ Kathleen M. Stafford,²
Rex K. Andrew,² and Robert I. Odom²

¹School of Oceanography, University of Washington, Seattle, Washington 98195;
email: wilcock@u.washington.edu

²Applied Physics Laboratory, University of Washington, Seattle, Washington 98105;
email: stafford@apl.washington.edu, rex@apl.washington.edu, odom@apl.washington.edu

Annu. Rev. Mar. Sci. 2014. 6:117–40

First published online as a Review in Advance on
July 17, 2013

The *Annual Review of Marine Science* is online at
marine.annualreviews.org

This article's doi:
10.1146/annurev-marine-121211-172423

Copyright © 2014 by Annual Reviews.
All rights reserved

Keywords

acoustics, ocean waves, earthquakes, marine mammals, shipping

Abstract

Very-low-frequency sounds between 1 and 100 Hz propagate large distances in the ocean sound channel. Weather conditions, earthquakes, marine mammals, and anthropogenic activities influence sound levels in this band. Weather-related sounds result from interactions between waves, bubbles entrained by breaking waves, and the deformation of sea ice. Earthquakes generate sound in geologically active regions, and earthquake T waves propagate throughout the oceans. Blue and fin whales generate long bouts of sounds near 20 Hz that can dominate regional ambient noise levels seasonally. Anthropogenic sound sources include ship propellers, energy extraction, and seismic air guns and have been growing steadily. The increasing availability of long-term records of ocean sound will provide new opportunities for a deeper understanding of natural and anthropogenic sound sources and potential interactions between them.

Noise (or sound)

level: total acoustic power expressed in decibels relative to a reference level, usually normalized by the bandwidth to yield a spectral density expressed in decibels; in water, the reference is $1 \mu\text{Pa}^2/\text{Hz}$

Mode: a characteristic harmonic acoustic response; a weighted sum of modes can be used to model the full acoustic field in the ocean

Range: the magnitude of a horizontal offset

1. INTRODUCTION

Because sound waves propagate efficiently in water and electromagnetic waves do not, sound plays an important role in facilitating remote interactions in the ocean. Humans use ocean sound for communication and for imaging the ocean’s interior, seafloor, and underlying crust. Sound is also a by-product of many anthropogenic activities in the ocean. Marine mammals use sound for communication and for echolocation.

The interval from 1 to 100 Hz coincides approximately with a frequency band that in ocean acoustics is termed the very-low-frequency (VLF) band. Because the wavelength of VLF sounds can be a significant fraction of the ocean depth, sound interactions with the seafloor are complicated, and their treatment requires an understanding of both acoustics and seismology. VLF sounds undergo little attenuation in water and thus propagate over large distances when trapped in the ocean waveguide. Sound levels are influenced over large regions by anthropogenic activities and marine mammals as well as by natural weather and geological processes. Records of VLF sounds from hydrophones and ocean-bottom seismometers are thus of multidisciplinary interest.

In this article, we aim to provide a broad review of scientific investigations of VLF sounds in the ocean. Section 2 presents an overview of the theory of acoustic propagation and the complications that arise at VLF frequencies from interactions with the seafloor. Section 3 then discusses the observation of sounds using hydrophones and seismometers. Sections 4–7 examine in turn the VLF sounds created by weather, earthquakes, marine mammals, and anthropogenic activities. Section 8 briefly discusses the interactions between low-frequency anthropogenic sounds and marine mammals and the difficulties associated with conducting robust studies to assess anthropogenic impacts. We conclude in Section 9 by outlining future research directions and needs.

2. THEORY

2.1. Acoustic Propagation

Typically, ocean acoustic propagation is a waveguide problem: The surface and bottom boundaries are much closer than any “side” boundary. The acoustic field $\psi(\mathbf{r}, t)$ as a function of space vector \mathbf{r} (representing $x, y,$ and z positions) and time t can therefore be decomposed into vertically trapped modes. If $\psi(\mathbf{r}, t)$ is decomposed into separate frequency components at Fourier (radian) frequency ω , the propagation of each component $\psi_\omega(\mathbf{r})$ is then governed (Munk et al. 1995, Brekhovskikh & Lysanov 2003) by the Helmholtz equation

$$\nabla^2 \psi_\omega(\mathbf{r}) + \frac{\omega^2}{c^2(\mathbf{r})} \psi_\omega(\mathbf{r}) = 0, \tag{1}$$

with appropriate boundary conditions at the ocean surface (where ψ is zero) and at the bottom (where the boundary condition is more complicated) (see Section 2.2). The dominant features of propagation are controlled by the sound-speed field $c(\mathbf{r}) = c_0(\mathbf{r}) + \delta c(\mathbf{r}, t)$, which may be decomposed conceptually into an average field $c_0(\mathbf{r})$ and a space/time-fluctuating part. The fluctuating part is usually much smaller than the average field and has timescales considerably longer than acoustic timescales, and it therefore has no significant role in the dominant features of propagation (Flatté et al. 1979, pp. 44–46).

For an ocean with properties that depend only on depth z , the acoustic field depends only on the range and depth. In this case, $c_0(\mathbf{r}) = c(z)$, the Helmholtz equation separates in depth and range, and the vertically trapped modes $\phi(z)$ obey the depth-only equation

$$\frac{\partial^2}{\partial z^2} \phi(z) + k_v^2 \phi(z) = 0, \tag{2}$$

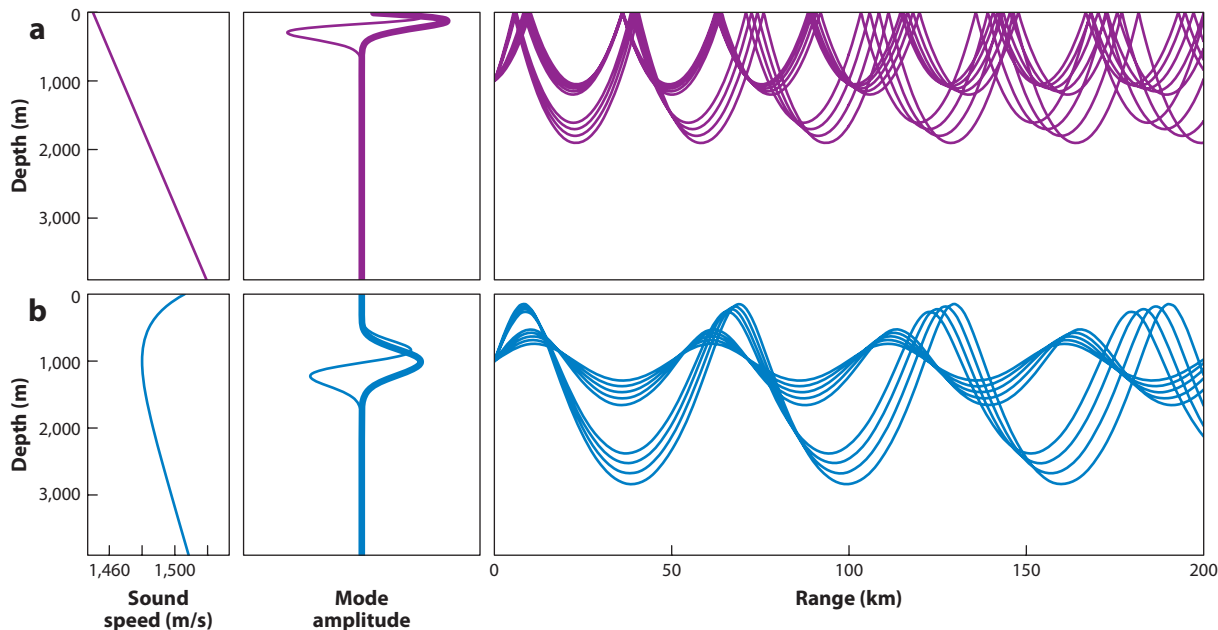


Figure 1

Two representative propagation regimes. (a) Polar regime. The left panel shows an idealized polar sound-speed profile, the middle panel shows modes 1 and 2 at 50 Hz (with mode 1 in *bold*), and the right panel shows two bundles of rays launched from an acoustic source at 1,000-m depth. The rays continually refract upward and skip off the surface. (b) Low-latitude regime. The left panel shows an idealized low-latitude sound-speed profile, the middle panel shows modes 1 and 2 at 50 Hz (with mode 1 in *bold*), and the right panel shows two bundles of rays launched from a source at 1,000-m depth. The rays cycle in the deep sound channel without interacting with the boundaries.

where k_v is the local vertical wavenumber (Munk et al. 1995). Each Fourier component can then be written as a weighted sum of all propagating modes.

Etter (2003, pp. 135–51) suggested that mode-theoretic models for shallow-water propagation become too computationally intensive above approximately 500 Hz. Very crudely, for a typical shallow depth H of 100 m and an average sound speed of 1,500 m/s, this frequency yields a value of roughly 30 for the nondimensional ratio H/λ of ocean depth to average acoustic wavelength λ . This ratio can indicate a practical transition from mode-theoretic to ray-theoretic propagation regimes. At higher frequencies (i.e., larger values of H/λ), the field can be visualized using rays (Munk et al. 1995), where rays indicate the sound propagation paths. The Helmholtz equation, in the high-frequency limit, yields ray equations that can be integrated forward for any $c_0(\mathbf{r})$, which makes ray diagrams particularly useful in regions with complex, range-dependent oceanography. For frequencies below 100 Hz in shallow water, mode representations are usually required. In the deep ocean, the transition ratio threshold is reached at approximately 10 Hz, which implies that higher VLF frequencies are adequately represented with ray diagrams.

The ocean's stratification makes $c_0(\mathbf{r})$ a strong function of depth but a weak function of range. Sound speed increases with hydrostatic pressure and temperature. Consequently, in isothermal and isohaline water, the sound speed increases with depth. A nearly isothermal example is the polar profile in **Figure 1a**, where surface and abyssal temperatures are similar. Alternatively, at low latitudes, solar heating of surface waters introduces a prominent temperature gradient; temperature decreases significantly with depth down to approximately 1,000 m and then decreases more slowly

Mode-theoretic:

a mathematical formalism that describes the acoustic field with modes

Ray-theoretic:

a mathematical formalism that conceptualizes the acoustic field with rays

Ray:

a path along which an acoustic or seismic signal travels

P wave: a longitudinal elastic body (or sound) wave in the Earth

S wave: a transverse elastic body wave in the Earth

Elastic anisotropy: elastic properties that are dependent on direction

in the deep ocean. Sound speed is also proportional to temperature; in the upper ocean, the temperature effect dominates the pressure effect, and sound speed decreases with increasing depth. Pressure and temperature exchange dominant roles at approximately 1,000 m, producing a sound-speed minimum (**Figure 1b**); below this depth, sound speed increases with depth as in a polar profile.

Figure 1 also shows the first few modes for both profiles. The lowest mode is concentrated near the surface for the polar profile and around the sound-speed minimum for the low-latitude profile (Munk et al. 1995). The ray picture for the polar profile shows propagation paths that continuously refract upward and bounce off the surface. In the low-latitude profile, fields initially refract downward until, significantly below the sound-speed minimum, they refract upward. The polar profile essentially ducts the sound along the surface, whereas the low-latitude profile ducts the sound about the deep sound-speed minimum. The deep duct is called the deep sound channel, or the sound fixing and ranging (SOFAR) channel (Urick 1983, p. 159).

2.2. Bottom Interaction

The bottom boundary between the ocean and the underlying crust is acoustically complicated. Much of the seafloor is sedimented with relatively muted topography, but near oceanic spreading centers, along continental margins, and in other volcanically and tectonically impacted regions, the topography can be rough. The properties of seafloor sediments and volcanic crust vary substantially with depth beneath the seafloor and can display substantial lateral heterogeneity. Energy from the acoustic wave field that interacts with the seafloor can be scattered, radiated into and out of the bottom, and absorbed by attenuation.

In the high-frequency limit, an acoustic wave with a planar wave front that is incident on a flat homogeneous sea bottom partitions into a reflected acoustic wave and transmitted compressional and shear body waves with amplitudes and phases given by the Zoeppritz equations (Ikelle & Amundsen 2005, pp. 92–95), which are dependent on the incidence angle and the seismic properties of the sea bottom. However, in the VLF band, the accuracy of these equations is limited even in areas of uniform seafloor, because wave-front curvature can be significant and the primary (P) and shear (S) wave velocities increase significantly with depth on the scale of the seismic wavelength (Ewing et al. 1992). Acoustic energy also couples into interface waves known as Scholte waves, which propagate along the seafloor and decay exponentially away from the boundary (Scholte 1947). At low frequencies, Scholte waves account for a large component of ocean noise near the seafloor (Nolet & Dorman 1996). Both P and vertically polarized S head waves (often referred to as lateral waves in the acoustics literature) propagate at the boundary and radiate into the water column (Brekhovskikh & Lysanov 2003).

The bottom boundary is further complicated by range dependence in the seafloor bottom/subbottom regions (Stone & Mintzer 1962, Smith et al. 1992). Fluctuations in acoustic wave speed can induce ray chaos in the water column that results in range-dependent waveforms (Smith et al. 1992, Tanner & Sondergaard 2007, Virovlyansky 2008). However, in shallow-water environments, the common causes of range dependence are related to the properties of the seafloor and the material beneath it. Variations in sediment composition and thickness, nonplanar boundaries, rough surfaces, strong density or velocity contrasts, and/or variations in water depth (Holland 2010) all add to the complexity of acoustic interactions with the seafloor. Even in areas of relatively simple geology, sediments can impose considerable range dependence on sound transmission over short ranges (Stoll et al. 1994).

Another source of complexity is elastic anisotropy, which is defined as the variation of elastic properties with direction. Possible sources of elastic anisotropy are the alignment of cracks and/or pores, preferred orientation of mineral grains, and lamination as a result of compositional layering

(Carlson et al. 1984, Koesoemadinata & McMechan 2004, Valcke et al. 2006). Although many authors favor a ray-based approach to modeling range dependence within the water column, the elastic properties of anisotropic sediments require properly simulating polarization effects. In sedimentary layers, compressional (P) and vertically and horizontally polarized shear (SV and SH) waves combine to form propagating modes (Koch et al. 1983, Stoll et al. 1994, Godin 1998). Anisotropy induces these seismic modes to mix the polarizations of P, SV, and SH motions, even in the absence of range dependence in the media (Park 1996, Soukup et al. 2013).

The simplest model for anisotropy is associated with an axis of symmetry (Backus 1962) and is a natural model in the presence of layering or aligned planar cracks or pore spaces. Marine sediments often have transversely isotropic elastic symmetry, with fast velocity directions in the plane parallel to the bedding plane and slow velocity directions along the normal of the bedding plane. Horizontal bedding leads to a transverse-isotropic geometry with a vertical symmetry axis. This orientation does not couple acoustic signals with SH waves. Such coupling does occur with a horizontal symmetry axis that can be produced by the introduction of vertical parallel cracks. Layered sediments with nonhorizontal bedding require a tilted symmetry axis whose orientation may vary vertically in cross-bedded sediments (Martin & Thomson 1997).

2.3. Attenuation

Propagating sound loses energy along its path by volume attenuation and volume and boundary scattering. Volume attenuation converts acoustic motion into heat primarily via bulk viscosity, owing principally to the presence of boric acid (Clay & Medwin 1977, pp. 96–102). For VLF sound, the attenuation is

$$\alpha(f) = (1.2 \times 10^{-7}) f^2 \text{ dB/km}, \quad (3)$$

where f is in hertz and is extremely low.

The acoustic impedance mismatch between seawater and seafloor sediment is often small, allowing a significant proportion of sound to propagate into the bottom. Attenuation levels are difficult to measure in the shallow subseafloor. They are likely frequency dependent and quite high, resulting in a loss of several decibels per kilometer for a 10-Hz signal; a significant portion of the sound propagating into the bottom does not radiate back out in the water column.

Scattering from rough boundaries also contributes to attenuation. The ratio of roughness scale to wavelength controls the amount of attenuation (Brekhovskikh & Lysanov 2003). Sea-surface roughness is negligible for VLF frequencies, but seafloor roughness such as undersea ridges and seamounts can be considerable, and further volume scattering occurs from heterogeneities beneath the seafloor. Although impedance contrast between seawater and basalt is relatively large, leading to reflected amplitudes that are higher than those in sedimented regions, the volcanic seafloor tends to be rough, and so much of the reflected energy is scattered.

In summary, fields ducted in the deep sound channel that avoid both the top and bottom experience only volume attenuation in the ocean and can propagate very long distances with very low loss. Sound fields that interact with the seafloor rapidly gain complexity but also undergo significant attenuation from scattering and absorption in the seafloor that limits their propagation distance.

3. OBSERVATIONS

Sounds in the ocean are detected with hydrophones that utilize piezoelectric transducers to generate electricity in response to pressure changes over a broad range of frequencies. Sounds can also be detected at the seafloor using three-component seismometers, in which each component records the velocity of the ground in one direction based on measurements of the motion or force required

SV wave: an S wave polarized in the vertical plane

SH wave: an S wave polarized in the horizontal plane

Decibel: a unit that describes differences in the power of acoustic signals (equal to 10 times the logarithm to base 10 of the ratio of the powers)

to restrain an internal mass attached to a frame by springs. Recently, considerable effort has gone into extending the sensitivity of ocean-bottom seismometers to frequencies well below 1 Hz, but the technology to detect seismic signals on the seafloor in the VLF band is well established.

Most recordings of ocean sound by the academic community are presently made with autonomous instruments. Hydrophones are routinely deployed near the seafloor and on moorings within the water column, and more recently have been attached to drifters and autonomous underwater vehicles. Depending on the application, they may be deployed singly, in compact directional arrays, or in broadly spaced networks. Ocean-bottom seismometers are typically deployed in sites of geological interest, such as continental margins and tectonic plate boundaries. They are usually deployed in networks with an instrument spacing that may vary from ~ 1 km to ~ 100 km. The number of ocean-bottom seismometers in use by the academic community has grown significantly over the past decade, and there are presently upward of 1,000. As a result of advances in low-power electronics and digital storage, it is now relatively straightforward to record acoustic or seismic signals autonomously in the VLF band for a year or more. However, for hydrophone instruments designed to also record much higher frequencies, storage capacity limitations often mandate shorter deployments, duty cycling, or event detection.

Although deployments with a sea-surface expression can return data by satellite, the data rates are sufficiently high that continuous streams of VLF data are best supported by cables. The US Navy has operated the cabled Sound Surveillance System (SOSUS) networks of hydrophones in the Atlantic and Pacific Oceans and local hydrophone networks in test ranges since the 1960s. Following the end of the Cold War, SOSUS became available for scientific applications (Fox & Hammond 1994, Nishimura & Conlon 1994), but the data remain classified. A number of real-time hydrophones have also been deployed over the past 15 years at several locations in the oceans as part of the International Monitoring System of the Comprehensive Nuclear-Test-Ban Treaty (Hanson et al. 2001). An important development in recent years has been the establishment of deepwater cabled observatories for research operations. These include the North-East Pacific Time-Series Undersea Networked Experiments (NEPTUNE) Canada (Barnes & Tunnicliffe 2008) and Ocean Observatories Initiative Regional Scale Nodes (Delaney & Kelley 2013) observatories in the northeast Pacific, the European Sea Floor Observatory Network (ESONET) (Priede & Solan 2002), and the Dense Ocean Floor Network System for Earthquakes and Tsunamis (DONET) off Japan (Kawaguchi et al. 2008). Most of these systems are multipurpose, and nearly all include a hydrophone or seismic monitoring capabilities. The potential exists to use abandoned submarine cables to make observations in remote locations (Butler et al. 2000, Kasahara et al. 2006) or to install telecommunications cables for dual scientific and commercial use.

4. WEATHER

Weather has a considerable influence on VLF sound. Surface winds, both near and far, transfer energy into the sea surface and generate sound through several mechanisms. Radiative transfer of heat to and from the upper ocean moderates propagation conditions, which can cause long-range ducting of sound (see Section 2). Surface cooling can also cause the formation of sea-surface ice, which has its own distinctive acoustic signature. Carey & Evans (2011, pp. 54–97) provided a recent comprehensive treatment of the effects of weather on VLF sound. The following sections review the dominant influences of surface wind waves and ice.

4.1. Surface Wave Interactions

Surface winds act on the sea surface to build gravity waves. Nonlinear interactions of surface gravity waves traveling in opposite or nearly opposite directions generate an acoustic signal at twice the

frequency of the surface waves (Longuet-Higgins 1950). The sound level in the upper few hundred meters can be substantially higher than at greater depths because the generation mechanism includes a near-field term (Cato 1991). When the signals propagate beneath the seafloor, they are termed microseisms. The microseisms from the longest-period swell waves corresponding to large storms propagate efficiently around the Earth, resulting in a prominent global peak in seismic noise levels centered between 0.1 and 0.2 Hz (Webb 1998). At higher frequencies, the amplitudes of microseisms decrease, because the amplitudes of ocean wave-height spectra decrease with frequency and higher-frequency seismic signals are attenuated over shorter distances within the Earth. Above 1 Hz, the noise is generated locally, and noise levels measured in the ocean and on the seafloor are closely correlated with the local wind speed up to a saturation threshold (Dorman et al. 1993, McCreery et al. 1993, Webb 1998).

Microseismic noise showing a characteristic decrease in amplitude with frequency dominates the spectra in **Figure 2** at frequencies up to approximately 5 Hz, with intervals of low noise

Microseisms: seismic noise created by the nonlinear interaction of ocean waves (the term was coined before the mechanism was known)

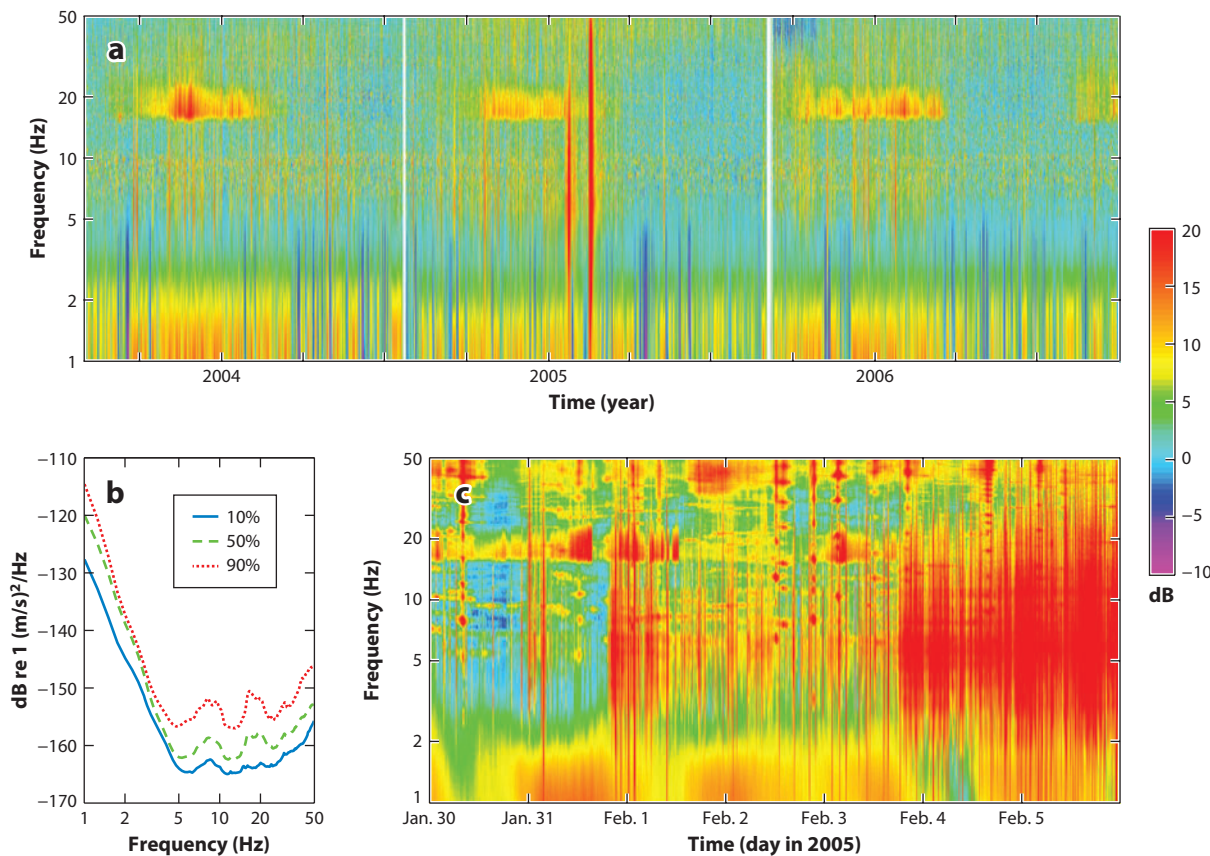


Figure 2

Seismic data collected in the very-low-frequency (VLF) band on the vertical channel of an ocean-bottom seismometer at 2,200-m depth on the Endeavor segment of the Juan de Fuca Ridge (Weekly et al. 2013). (a) Three-year velocity spectrogram. Each vertical raster line is a spectrum estimate averaged over 24 h. The 10th-percentile curve at each frequency has been removed to enhance the dynamic range. Two gaps mark annual servicing. (b) The 10th-, 50th-, and 90th-percentile curves. (c) Detailed spectrogram for one week in 2005 that includes a seismic swarm on the Juan de Fuca Ridge. The time-axis resolution is 10 min. Measurements are bounded at 50 Hz owing to the sampling rate.

corresponding to intervals of calm. The contribution from this mechanism may even extend to higher frequencies: Acoustic pressure spectra measured at the seafloor in deep regions of the North Pacific have features that can be matched to the spectra of ultragravity waves up to 30 Hz or more (Duennebieer et al. 2012, Farrell & Munk 2013).

4.2. Surface Waves: Bubbles

When ocean waves break owing to instability mechanisms and then form (depending on the size of the wave) microbreakers, spilling breakers, or plunging breakers, the overturning fluid entrains air bubbles. Air bubbles are like simple mass-spring systems, with the highly compressible interior air acting like a spring and the fluid outside the bubble acting like a mass. Once excited, bubbles “ring” with characteristic oscillation frequencies f proportional to their radius, according to the Minnaert (1933) formula

$$f = \frac{1}{2\pi R} \left(\frac{3\gamma P}{\rho} \right)^{\frac{1}{2}}, \quad (4)$$

where R is the bubble radius, P is the ambient pressure, ρ is the liquid density, and γ is the ratio of specific heats for air. Optical (Johnson & Cooke 1979, Deane 1997) and indirect acoustic resonance (Breitz & Medwin 1989, Farmer et al. 1998) measurements showed that the sizes of injected bubbles range from less than 20 μm to several centimeters; these bubbles consequently contribute to ambient sound at ringing frequencies of several hundred hertz to several hundred kilohertz.

Bubble entrainment and subsequent bubble ringing are therefore an accepted source mechanism for noise above the VLF range. Evidence supporting mechanisms that could generate noise within the VLF range is less decisive. Measurements are difficult owing to the pervasive contamination of anthropogenic noise (see Section 7). Nevertheless, studies in the Southern Hemisphere, where ship traffic is sparse (see Section 7.1), have found good correlation between local sound levels and wind speed (Cato 1976, Burgess & Kewley 1983). Because sea-surface energetics (whitecapping, gravity wave height, etc.) are related to wind forcing, these and similar studies dictate that source mechanisms be associated with sea-surface processes. Ultragravity surface waves (Section 4.1) provide at best a possible mechanism over only the lower end of the VLF range. Theories proposing individual ringing bubbles are discounted because bubbles with sizes large enough to resonate below 100 Hz have not been observed. An alternative theory proposes that the entire volume of bubbly fluid injected by a single breaking wave acts itself like one big bubble (Carey & Browning 1988, Yoon et al. 1991), with a corresponding resonance frequency much lower than that of its much smaller constituent bubbles.

Near coastlines, shoaling gravity waves generate considerable sound levels while breaking. Bubble oscillation is also a principal mechanism of sound generation here (Haxel et al. 2013). An auxiliary mechanism that can contribute acoustic energy over a broad frequency band is the current-induced transport of sediment (rocks, stones, and sand). Sound from shoaling waves breaking against a shoreline can propagate downslope away from the shore and out into open waters, and can make a significant contribution in coastal regions.

Weather effects are readily apparent at the higher VLF frequencies in the data captured near San Nicolas Island off the coast of Southern California (**Figure 3**). Above approximately 70 Hz, a prominent short-timescale striation pattern is evident. This signal correlates with (predominantly local) storms, which invoke bubble production via whitecapping and may persist for timescales of several days to a week.

Bannister (1986) has proposed high-latitude storms as a mechanism for generating distant sea-surface sound that can propagate to lower latitudes via the deep sound channel. At high latitudes,

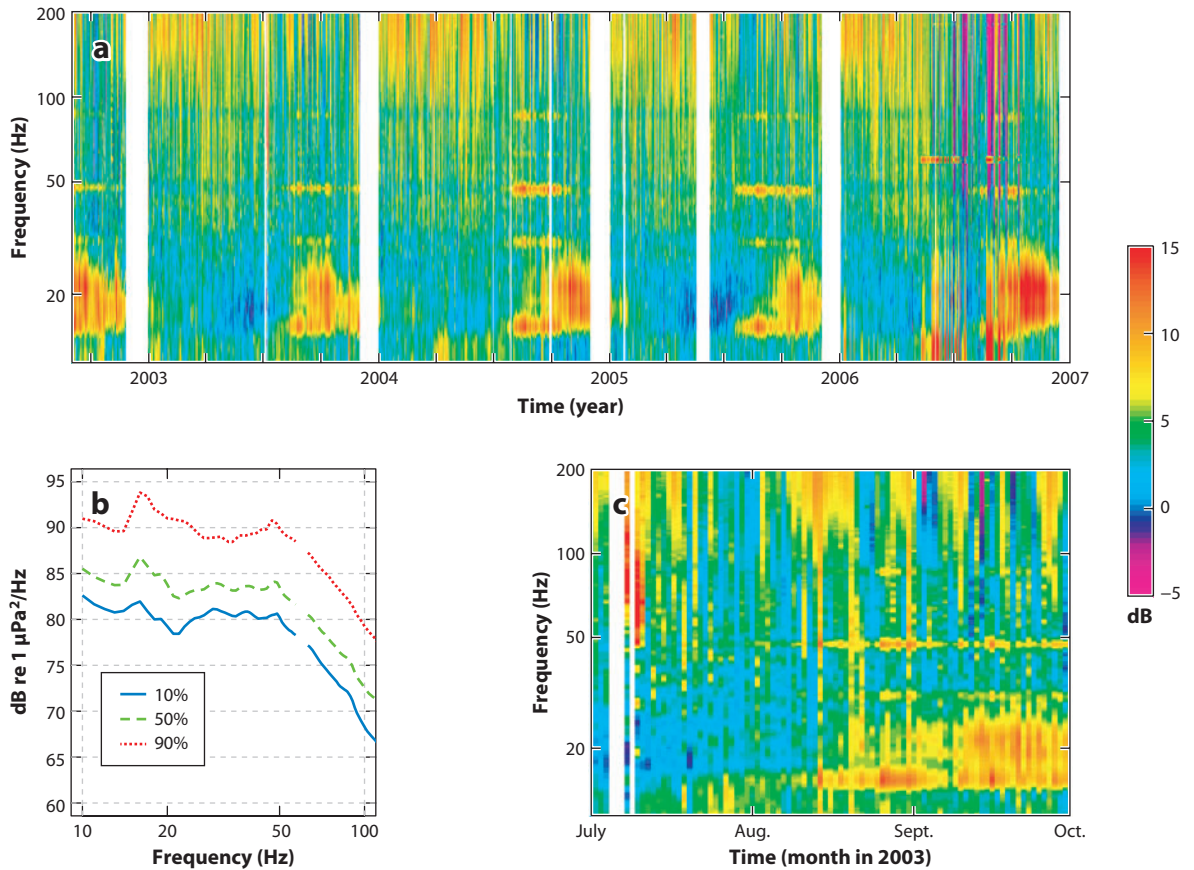


Figure 3

VLF sound collected off San Nicolas Island, Southern California (McDonald et al. 2006, Andrew et al. 2011). (a) Four-year spectrogram. Each vertical raster line is a spectrum estimate averaged over 24 h. The 10th-percentile curve at each frequency has been removed to enhance the dynamic range. Gaps represent equipment outages. (b) The 10th-, 50th-, and 90th-percentile curves. (c) Detailed spectrogram for several months in 2003. The time-axis resolution is 24 h. Measurements are bounded at 10 Hz owing to instrumentation calibration uncertainty at lower frequencies.

the deep sound channel is essentially at the surface, but it deepens toward the equator. At low latitudes, this provides a duct for confining the sound of distant surface energy to subsurface regions below a potentially quieter layer. Sufficiently accurate measurements do not yet exist to support this hypothesis.

4.3. Ice

Although the ice-covered Arctic would be expected to experience very low ambient noise levels owing to the lack of wind-driven waves, the dynamics of sea ice—including ice formation and deformation, pressure ridging, and cracking—greatly increase ambient noise levels over a broad range of frequencies (Lewis & Denner 1988, Farmer & Xie 1989). Below 100 Hz, ice cracks and fractures (**Figure 4a**) caused by wind and stress contribute significantly to ambient noise levels, particularly in winter and spring months in ice-covered oceans (Dyer 1988, Roth et al. 2012).

In the Antarctic, noise from rifting and breaking of icebergs in the frequency band from 2 to 35 Hz has been detected thousands of kilometers away from the event source, suggesting that these events have high sound source levels (~ 245 dB re 1 μPa at 1 m) (Chapp et al. 2005, Gavrilov & Li 2008). Other acoustic signals from icebergs include harmonically rich tremors with fundamental frequencies between 4 and 10 Hz. These so-called variable harmonic tremors can last from hours to days and have been associated with the movement of very large icebergs (Chapp et al. 2005). Shorter-duration low-frequency signals (so-called cusped pulse tremors, from 4 to 80 Hz) that are more pulsive and last only minutes to hours have been attributed to the internal resonance of smaller icebergs (Chapp et al. 2005). Low-frequency resonance may occur only when two icebergs collide or when very large icebergs ground on the ocean floor (Talandier et al. 2002). A further source for low-frequency sounds coming from the open ocean is internal resonance that occurs as very large icebergs are displaced when they encounter large eddies or the polar or sub-Antarctic fronts (Talandier et al. 2006). All of these signals from icebergs in the Southern Ocean can dominate low-frequency noise spectra at long distances (Chapp et al. 2005, Talandier et al. 2006).

Sound source level:

the intensity of sound sources expressed in decibels relative to a reference sound measured at or corrected to a specific range; in water, the reference is 1 μPa at 1 m

T wave: a body wave from an earthquake that travels as a ducted wave in the ocean sound channel

5. EARTHQUAKES

Earthquakes are a significant source of discrete VLF sounds in the ocean; they are observed both as body waves that are transmitted across the seafloor at steep angles and as ducted waves known as T waves, which can propagate long distances horizontally within the sound channel. The spectrum of a seismic body wave reaching the seafloor is dependent on the earthquake source characteristics and the attenuation that occurs as the elastic wave propagates through the Earth (Shearer 2009, pp. 181–83). Earthquake signals in the VLF band are characterized by decreasing amplitudes at higher frequencies for two reasons. First, destructive interference reduces radiated amplitudes for frequencies exceeding a corner frequency that is approximately equal to the wave speed divided by the dimensions of the fault. Typical corner frequencies range across the VLF band from ~ 1 Hz for a magnitude-5.5 earthquake to ~ 100 Hz for a magnitude-1.5 microearthquake. Second, anelastic attenuation along the propagation path increases approximately linearly with frequency. Although shear (S) waves tend to have higher amplitudes at the source than compressional (P) waves, they are usually attenuated more strongly within the Earth and thus are observed at lower frequencies.

Body waves from teleseismic (distant) earthquakes are often not observed in the VLF band. Two notable exceptions are the P_n and S_n phases, which propagate with little attenuation in the lithosphere of oceanic plates and can be observed at frequencies extending to 20–30 Hz and distances up to 3,000 km (Walker 1981, Walker et al. 1983). Otherwise, the detection of body waves in the VLF band is limited to P waves near 1 Hz and is dependent on the characteristics of

Figure 4

Examples of waveforms and spectrograms for various transient very-low-frequency (VLF) signals. The waveforms have been filtered with a 5-Hz high-pass filter, and the spectrograms have been normalized to the 5th-percentile value in the plotted frequency band. All but panel *b* are for an 80-s time interval, but the bandwidth and scaling of the spectrograms vary between signals. (*a*) Ice cracking noise recorded by a hydrophone. (*b*) A magnitude-4 earthquake recorded by an ocean-bottom seismometer at a 30-km range, showing P-, S-, and T-wave arrivals. (*c*) A swarm of local microearthquakes recorded by an ocean-bottom seismometer. The P- and S-wave arrivals are closely spaced for each earthquake, and two water column reverberations (labeled WCR) are visible for each earthquake spaced approximately 3 s apart. (*d*) A T wave for a distant earthquake recorded by a hydrophone. (*e*) The A and B calls of a northeast Pacific blue whale recorded by a hydrophone. (*f*) Regularly spaced 20-Hz fin whale pulses recorded by an ocean-bottom seismometer. Both the direct arrival and first water column reverberation are visible. (*g*) Air-gun shots spaced 18 s apart recorded on a hydrophone, showing multiple shallow-water reverberations. (*h*) Ship noise recorded by a hydrophone.

the earthquake and ambient noise levels (Webb 1998). Ocean-bottom seismometer experiments in some locations may fail to record any teleseismic P waves at ≥ 1 Hz (Wilcock et al. 1999).

Because they propagate over shorter distances and thus undergo less attenuation, local earthquakes near a receiver are a more significant source of VLF sounds than earthquakes at larger ranges. P and S waves are recorded by seafloor seismometers (**Figure 4b,c**), and the P waves are transmitted as coherent sound into the ocean. Because most earthquakes concentrate along tectonic plate boundaries, the number of local earthquakes is highly dependent on location. Seismic networks deployed on oceanic spreading centers (Tolstoy et al. 2006) and transforms (McGuire et al. 2012) may record tens of thousands of earthquakes per year. During earthquake swarm events, earthquakes and tremor can be the dominant sources of VLF noise (Tolstoy et al. 2006). In **Figure 2**, two large regional swarms are apparent in early 2005.

In most of the ocean, T waves are the most common earthquake sound (**Figure 4d**). T waves are characterized by emergent waveforms and are generated by two mechanisms. In regions with an inclined seafloor, such as continental slopes and the flanks of seamounts, successive reverberations between the sea surface and the seafloor propagating downslope lead to a progressive reorientation of acoustic rays toward the horizontal (Johnson et al. 1963, Okal 2008). This can lead to the generation of T waves that propagate into the ocean basin from sites on the seafloor that may be hundreds of kilometers away from the earthquake epicenter. In the absence of large-scale bathymetric features, abyssal T waves can be generated near an earthquake epicenter by scattering from seafloor roughness (Fox et al. 1994, de Groot-Hedlin & Orcutt 2001a, Park et al. 2001).

Because T waves propagate large distances in the ocean, they provide a means to monitor seismicity in the oceans using hydrophones at detection levels that are substantially lower than those of P and S waves recorded by the global seismic network. In the northeast Pacific, near-real-time analysis of data from the SOSUS network has provided a 20-year catalog of seismicity on the Juan de Fuca Plate (Dziak et al. 2011). One exciting result of this monitoring has been the real-time detection of several seafloor volcanic eruptions on the Juan de Fuca and Gorda Ridges (Fox et al. 1995, Dziak et al. 2011). This detection facilitated rapid ship-based responses that have contributed substantially to our understanding of seafloor spreading and subsurface hydrothermal and microbial processes (Delaney et al. 1998, Cowen et al. 2004). Regional networks of autonomous moored hydrophones have also been deployed in the deep sound channel in several other regions to create substantial catalogs of oceanic seismicity (Dziak et al. 2012).

6. MARINE MAMMALS

Marine mammals, particularly cetaceans (whales and dolphins), produce sounds over the largest range of any class of animal: from subsonic (large whales) to supersonic (porpoises and beaked whales) frequencies. The largest whales—the blue (*Balaenoptera musculus*) and fin (*Balaenoptera physalus*) whales—produce VLF sounds. Other species, such as humpback (*Megaptera novaeangliae*) and bowhead (*Balaena mysticetus*) whales, produce some sounds below 100 Hz, but these signals are only a small part of their acoustic repertoire. The sounds of blue and fin whales, by contrast, are almost all below 100 Hz. Both of these species produce long, loud bouts of calls, particularly in winter months, that contribute to overall regional ambient noise levels near 20 Hz (Curtis et al. 1999, Andrew et al. 2011, Nieu Kirk et al. 2012) (**Figures 2** and **3**). These long bouts, or songs, are thought to be male reproductive displays used to advertise fitness to other males, to attract females, or potentially to advertise a food resource (Payne & Webb 1971, Watkins et al. 1987, Croll et al. 2002, Oleson et al. 2007).

Blue whale calls (**Figure 4e**) generally consist of one to three units produced in a phrase, all of which have fundamental frequencies that are below 50 Hz and as low as 15 Hz. These units

are long (>10 s each) and may be frequency or amplitude modulated. Blue whale calls are also quite loud, with source level estimates ranging from 180 to 189 dB re 1 μ Pa at 1 m (Cummings & Thompson 1971, Thode et al. 2000, Širović et al. 2007). Although blue whale calls worldwide share these characteristics of being long, loud, and in the VLF band, whales from different areas produce sounds that are geographically distinctive (Stafford et al. 2001, 2011). The structure of blue whale songs remains stable over time, but there is evidence that the fundamental frequencies of the songs of some populations are decreasing, although a definitive reason for this decrease has not been found (McDonald et al. 2009, Gavrilov et al. 2012).

Fin whales also produce subsonic vocalizations (**Figure 4f**), but their calls are relatively short (1-s) pulses that are often slightly frequency modulated, spanning from \sim 40 down to 10 Hz. These “20-Hz pulses,” as they are known, are repeated every 10–40 s and, like blue whale calls, may continue for hours or days at a time (Watkins 1981, Watkins et al. 1987). Fin whale calls are loud; source levels from 171 to 189 dB re 1 μ Pa at 1 m have been reported (Watkins et al. 1987, Charif et al. 2002, Širović et al. 2007, Weirathmueller et al. 2013). There is some evidence that the timing between successive pulses may vary geographically, but relatively few studies have examined this (Delarue et al. 2009, Castellote et al. 2011). In addition, some fin whale populations produce a higher-frequency pulse that sometimes accompanies the 20-Hz pulses; the frequency of this appears to vary geographically (Širović et al. 2009, Simon et al. 2010).

Although blue and fin whales produce other signals besides song notes in different behavioral contexts, these tend to be higher frequency and are produced less often than songs, and they therefore contribute less to overall ambient noise levels. Two other cetacean species produce signals with fundamental frequencies below 100 Hz: sei (*Balaenoptera borealis*) and Bryde’s (*Balaenoptera edeni*) whales (Oleson et al. 2003, Rankin & Barlow 2007, Baumgartner et al. 2008). Relatively little is known about the acoustic behavior of these species, but the amplitudes of their signals are much lower than those of blue or fin whales, so these signals are unlikely to contribute significantly to global noise budgets (Cummings et al. 1986, Baumgartner et al. 2008).

7. ANTHROPOGENIC SOUNDS

Human utilization and exploitation of the ocean have resulted in additional components to VLF sound that did not exist before the nineteenth century. The usual catalog of sources includes at-sea structures, installations, and vessels; prominent categories are described below. Rarely considered—and poorly understood—are land-based sources. De Groot-Hedlin & Orcutt (2001b) suggested that sound from open-ocean acoustic sources could couple into the coastal crust and remain detectable some distance inshore. If the opposite is true (Collins et al. 1995), then the radiated noise from coastal cities might enter the marine soundscape. However, no definitive measurements exist, and this remains a speculative component.

7.1. Shipping Noise

One of the earliest uses of ambient sound was the passive detection of radiated noise from surface or subsurface vessels—a central military objective. Ships radiate a distinctive signal containing multiple harmonics over a diffuse broadband component (**Figure 4b**). The harmonics are related to the rotating machinery involved in the propulsion system: The fundamental frequency corresponds to the propeller blade rate, which is the rate that blades pass the shallowest depth (Ross 1976). For a propeller with N blades, this rate is N times the shaft rotation speed.

The primary noise mechanism appears to be cavitation occurring near the tip of the blade as the blade passes the top of its rotational arc (Ross 1976). The intensity of the radiated noise was

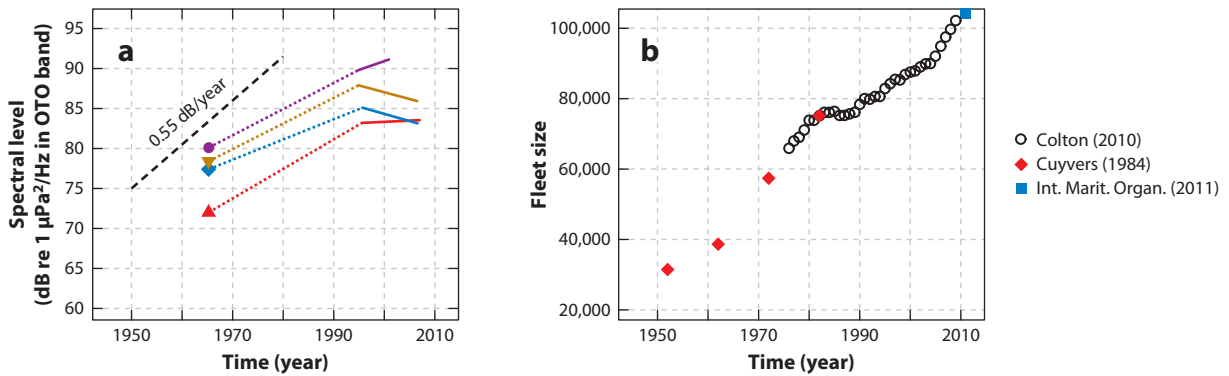


Figure 5

Merchant shipping contribution to acoustic noise. (a) Measurements at 32 Hz from four sites off the North American west coast. The symbols represent two-year averages at these sites from measurements made in the 1960s. The solid lines represent the durations and linear trends of a contemporary data set from the same sites (Andrew et al. 2011). Dotted lines connect the data from each site but are not intended to describe the ambient sound evolution during the intervening years. The dashed line with slope 0.55 dB/year is a linear regression described by Ross (1993) made from numerous measurements (not shown) at sites in the North Pacific and North Atlantic spanning roughly 1950–1970. (b) Size of the world merchant fleet over the same time period, compiled from several sources (Cuyvers 1984, Colton 2010, Int. Marit. Organ. 2011).

originally parameterized (using World War II ships) by ship speed and length (Ross 1976); recent studies (using newer ships) have suggested that ship draft, propeller size, and propeller tip depth might be better correlates (Wales & Heitmeyer 2002). Radiated levels are highly variable: Modern estimates of source level over 5–100 Hz for under-way vessels (Wales & Heitmeyer 2002, Leigh & Eller 2008, McKenna et al. 2012b) range from 171–190 dB re 1 $\mu\text{Pa}^2/\text{Hz}$ at 1 m for supertankers to 150–168 dB re 1 $\mu\text{Pa}^2/\text{Hz}$ at 1 m for small tankers, with levels decreasing with increasing frequency.

Early VLF sound observations (Wenz 1962) noted the signatures of individual passing ships, with amplitudes that increased as the ships approached and decreased as they receded. Wenz (1962) postulated that the ambient sound when a ship was not passing nearby was due to the distant armada of merchant ships, none of which were distinctly identifiable, and termed this contribution traffic noise. From a military perspective, this is the background noise that limits the performance of passive surveillance detection of hostile vessels. To first order, the size of the world’s merchant fleet should be a positively correlated indicator of this contribution. Indeed, Ross (1993) showed that traffic noise increased throughout the middle of the twentieth century, when economic growth fueled an increase in transoceanic shipping. Measurements off the California coast (Andrew et al. 2002, McDonald et al. 2006, Chapman & Price 2011) showed that distant shipping noise levels have risen by approximately 10 dB compared with early reports. Statistics have indicated that the world merchant fleet size continues to grow (**Figure 5**); however, more recent high-resolution measurements off the North American west coast (Andrew et al. 2011) showed shipping noise trends that are level or even slightly decreasing. The discrepancy is not understood. Ainslie (2011) suggested that sea-surface temperature and/or ocean acidification changes may be introducing seasonal and interannual patterns in long-term records. Further complicating the issue is strong regional evidence that economic downturns, new regulations, and shipping lane relocation may be responsible (Frisk 2012, McKenna et al. 2012a).

The total contribution from shipping depends in part on the distribution of near and distant ships. The distribution is most heavily weighted in the shipping lanes crossing the Northern

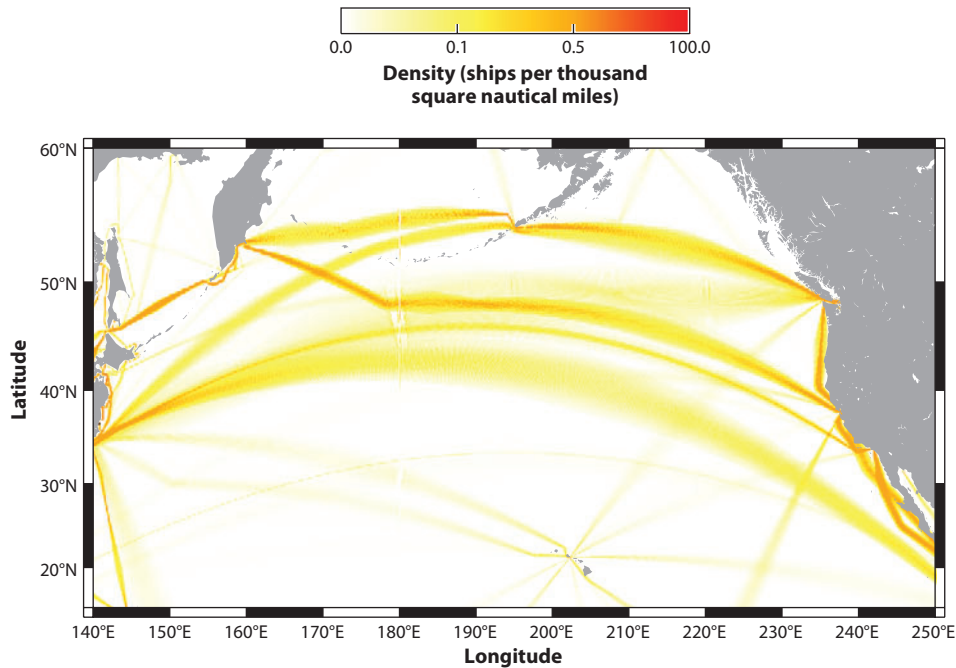


Figure 6

Shipping density in the North Pacific, compiled from 1998 records (Emery et al. 2001). The color scale is stretched at low densities to enhance trans-Pacific shipping lanes.

Hemisphere. **Figure 6** presents an estimate of ship density in the North Pacific for 1998 (derived from Emery et al. 2001). Shipping densities in the Southern Hemisphere are much lower, and the ship noise contribution there is much lower. Density maps such as **Figure 6** are key to understanding the spatial distribution of shipping noise and its regional impact on marine ecology, but density maps have been difficult and expensive to compile, and only two global maps have ever been constructed: one for 1998 (Emery et al. 2001) and one for 2010 (Walbridge 2013).

7.2. Energy Extraction

Civilization’s increasing demand for energy has prompted an expansion of efforts to extract energy from ocean resources. Oil drilling is a well-known example, and recent projects include wind farms and tidal turbines. The VLF sound contributions from these initiatives may be space/time limited (as with pile driving for wind farm towers or oil rig decommissioning) or chronic (as with routine service vessel transportation to and from existing oil rigs). Additionally, the contributions are generally not well understood, possibly because the spatial and temporal extent of the activities is not well documented (e.g., for oil rig service vessel sizes, speeds, schedules, and routes) or the technology is too new (e.g., for undersea turbines). Several examples are given below.

Wind farms are a popular contemporary “green energy” technology. Wind turbines installed in the ocean radiate sound into the water and seabed from their foundations via structure-borne vibration owing to gearbox noise and turbulence on the fan blades. As more offshore wind farms are built, this technology will become a permanent addition to the VLF soundscape. Tougaard et al. (2009) measured radiated noise levels from individual turbines in shallow water and often observed a peak near 25 Hz at levels of 100–120 dB re 1 $\mu\text{Pa}^2/\text{Hz}$.

Hydrokinetic (tidal) turbines are a very new technology, and radiated levels are not available because no at-sea installations exist yet. Zampolli et al. (2012) used aerodynamic and turbulence models to postulate that the primary noise mechanism will be dipole radiation from the fan blades owing to unsteady flows originating from structures upstream of the blades. Most of the radiated noise is predicted to be below 20 Hz, with a level at 100 m of up to 100 dB re $1 \mu\text{Pa}^2/\text{Hz}$ for a free stream velocity of 1.7 m/s.

Construction of wind farms, drilling platforms, and support infrastructure in harbors usually requires pile driving. The dominant radiation mechanism in impact pile driving is a Mach wave related to the radial expansion of the pile that propagates with supersonic speed down the pile after each impact (Reinhall & Dahl 2011). Typically, each impact radiates energy primarily above 100 Hz. Precise characterizations of source (or received) levels are generally not available owing to the vast differences in propagation conditions from site to site. Erbe (2009) reported sound exposure levels of 110–140 dB re $1 \mu\text{Pa}^2 \cdot \text{s}$ over 10–40 Hz at a range of 320 m from a pier construction site (water depth 1 m); Bailey et al. (2010) reported levels of 10–120 dB re $1 \mu\text{Pa}^2/\text{Hz}$ over 10–100 Hz at a range of 1,520 m during construction at an offshore (water depth 40 m) wind farm site.

7.3. Seismic Air Guns

An air gun generates an acoustic signal by releasing compressed air under high pressure from a pneumatic chamber. Arrays of air guns of different sizes can be tuned by adjusting their relative positions and discharge times to create an impulsive signal that is directed downward (Sheriff & Geldart 1995, pp. 211–18). A typical air-gun array signature (**Figure 4g**) extends across most of the VLF band, from a few hertz to well above 100 Hz. Air-gun arrays have high source levels; for example, the 36-element, 6,600-cubic-inch air-gun array on the R/V *Marcus G. Langseth* has a peak source level of 259 dB re $1 \mu\text{bar}$ at 1 m (Tolstoy et al. 2009). As a result, they can be recorded in the sound channel at distances of several thousand kilometers (Blackman et al. 2004; Nieuwkirk et al. 2004, 2012). During a seismic survey, they are discharged repetitively with an interval of ~ 20 s.

There are approximately 150 seismic survey vessels worldwide (*Offshore* 2012) that operate on the continental shelves and slopes of rifted continental margins. Seismic surveys are more common in the Atlantic than in the Pacific. Like energy extraction projects (Section 7.2), individual surveys are sporadic and depend on the proprietary exploration schedules of the petroleum companies, although the overall activity can be remarkably persistent in some regions (Nieuwkirk et al. 2012).

7.4. Ocean Science

In the late 1980s, ocean acousticians proposed an ocean temperature measurement technique that uses long-range VLF signals. Pilot programs (Munk & Forbes 1989, Dushaw et al. 1999, Worcester & Spindel 2005) injected controlled phase-modulated signals at 57–75 Hz into the deep sound channel. The experiments of the Acoustic Thermometry of Ocean Climate (ATOC) project documented that the variability in basin-scale low-frequency sound transmission is due to seasonal changes in ocean temperature (ATOC Consort. 1998). These changes in temperature in turn influence sea-surface height measurements owing to thermal expansion as seawater warms. This methodology of producing low-frequency signals that are loud enough to be detected across ocean basins has been used in the Arctic with a 20.5-Hz signal to detect basin-scale warming of more than 0.5°C from 1994 to 1999 (Mikhalevsky et al. 1999, Mikhalevsky & Gavrilov 2001).

8. INTERACTIONS BETWEEN ANTHROPOGENIC SOURCES AND MARINE MAMMALS

Assessing whether anthropogenic sound has a negative impact on marine mammals is extremely difficult. Our understanding of the hearing responses of many marine mammals, particularly large whales, is incomplete. Determinations of whether they can hear certain signals and how loud the signals must be to be heard are often based on the frequency range of signals the marine mammals produce and potentially those produced by their predators. Further, to monitor the impacts of anthropogenic sound on marine mammals, visual observations of animals at the surface are most often used. Visual observations are limited to daylight hours and good weather, animals at the surface within visual range (which is much shorter than acoustic range), and a limited number of behavioral cues (e.g., changes in swim speed or direction and changes in respiration rate). Many marine mammal species spend >90% of their time underwater, and therefore responses to sound that occur below the surface cannot be documented. Finally, we still know so little about the ecology and behavior of most marine mammals that unless an animal washes up on a beach with obvious signs of acoustic trauma, it is extremely difficult to determine how, and for how long, exposure to underwater sounds impacts marine mammals on an individual- or population-level scale.

Reports of the impacts (or lack thereof) of low-frequency sources are relatively few, are often observational rather than experimental, and may arrive at different conclusions. For instance, fin whales exposed to air-gun surveys in the Mediterranean Sea moved away from the area and remained away for some time after the surveys ceased (Castellote et al. 2012). Blue whales increased their calling rate, potentially to compensate for increased ambient noise levels (Di Iorio & Clark 2010). McDonald et al. (1995) and Dunn & Hernandez (2009), in contrast, found no evidence of changes in the call rates of blue whales tracked from 28 to 100 km away from active air-gun operations or in the behavior of blue and fin whales near active operations. The ATOC experiments (see Section 7.4) were controversial when first conceived: The impacts, particularly on marine life, of injecting basin-spanning VLF sound into the deep sound channel were unknown. At the time, VLF levels of merchant shipping, nearshore construction, and geophysical exploration, which are generally much higher than ATOC signals, were either unmeasured or not publicly available. Some studies showed that the signals caused little or no behavior modification in cetaceans (Au et al. 1997, Mobley 2005), whereas others found that individual humpback whales spent less time at the surface when exposed to ATOC signal playbacks, although the overall distribution of humpback whales in the area did not change (Frankel & Clark 1998, 2000).

Although determining the interactions between anthropogenic noise sources and marine mammal life histories is fraught with difficulty and cannot be distilled into generalizations, it is important to take into consideration when discussing low-frequency noise. It is clear that shipping noise in the Northern Hemisphere, at least, has been increasing steadily (see Section 7.1), and this noise reduces the range over which species that use low-frequency sounds can communicate (Clark et al. 2009, Hatch et al. 2012). Low-frequency ship noise has been implicated in increased levels of stress hormones in North Atlantic right whales (*Eubalaena glacialis*) (Rolland et al. 2012). Noise from oil and gas exploration is pervasive year-round in the North Atlantic (Nieukirk et al. 2012). Seismic air-gun pulses overlap the frequency bands used by blue and fin whales (Nieukirk et al. 2004). The cumulative impact of these sources of increasing VLF noise on marine species that use sound as the primary means of sensing their environment may disrupt vital life history events, and this disruption may not be immediately obvious (Hatch et al. 2012).

9. FUTURE DIRECTIONS

Although the military has been observing VLF sound in the oceans for 50 years, long-term records of sound in the ocean obtained with hydrophones or seafloor seismometers are still scarce in the public domain. Advances in the capabilities and numbers of autonomous recorders and, more important, the move to establish long-term ocean observatories promise to substantially change this. An increasing number of ambient sound observations will provide enormous opportunities but will also bring additional challenges regarding collection protocols, data quality, record formats, metadata, and ease of access. These problems have been largely resolved within the academic seismic community through the development of global waveform databases and the tools to access them [the Incorporated Research Institutions for Seismology (IRIS) Data Management Center; <http://www.iris.edu/data>]; a similar approach is desirable for ocean acoustics data.

The dual use of SOSUS hydrophone data (Fox & Hammond 1994, Nishimura & Conlon 1994) has demonstrated the utility of long-term acoustic monitoring for studying weather-related noise, earthquakes, marine mammals, and shipping noise, and such studies will expand with open-access data. Seafloor seismic networks are also increasingly used to study marine mammals (McDonald et al. 1995, Rebull et al. 2006, Dunn & Hernandez 2009, Soule & Wilcock 2012). One particularly important opportunity is the prospect of more extensive and systematic studies of the impacts of anthropogenic sound on marine mammals. In addition to acoustics data, such studies will require assessing the contributions from a wide variety of existing transient and chronic anthropogenic sources. One such effort (Natl. Ocean. Atmos. Adm. 2012, Porter & Henderson 2013) required the integration of multiple databases for large commercial vessels, cruise ships, and roll-on/roll-off ferries, coupled with seismic survey track lines as stipulated in oil and gas exploration permits, service vessel activity models from government projection reports, and pile-driving noise models from environmental impact assessments for predictions in the US exclusive economic zone. The difficulties of assembling such data will only increase as the number and types of sources expand.

A global approach to handling ocean acoustics data is clearly needed, and the Sloan Foundation recently initiated such an effort. Denoted the International Quiet Ocean Experiment (Boyd et al. 2011), this project can perhaps serve as a framework for international collaboration in monitoring global ambient sound and estimating its effects on the acoustic ecology of the world's oceans.

DISCLOSURE STATEMENT

The authors are not aware of any affiliations, memberships, funding, or financial holdings that might be perceived as affecting the objectivity of this review.

ACKNOWLEDGMENTS

The authors thank Ross Chapman, Doug Cato, and an anonymous reviewer for insightful reviews. Funding for this work has come in part from the Office of Naval Research (grants N00014-08-1-0523 to W.S.D.W., N00014-13-1-0009 to R.K.A., and N00014-11-1-0208 to R.I.O.) and the National Science Foundation (grant OCE-0937006 to W.S.D.W.).

LITERATURE CITED

- Ainslie M. 2011. Potential causes of increasing low frequency ocean noise levels. *Proc. Meet. Acoust.* 12:070004
Andrew RK, Howe BM, Mercer JA. 2011. Long-time trends in low-frequency traffic noise for four sites off the North American west coast. *J. Acoust. Soc. Am.* 129:642–51

- Andrew RK, Howe BM, Mercer JA, Dzieciuch MA. 2002. Ocean ambient sound: comparing the 1960s with the 1990s for a receiver off the California coast. *Acoust. Res. Lett. Online* 3:65–70
- ATOC Consort. 1998. Comparison of acoustic tomography, satellite altimetry, and modeling. *Science* 281:1327–32
- Au WWL, Nachtigall PE, Pawloski JL. 1997. Acoustic effects of the ATOC signal (75 Hz, 195 dB) on dolphins and whales. *J. Acoust. Soc. Am.* 101:2973–77
- Backus GE. 1962. Long-wave elastic anisotropy produced by horizontal layering. *J. Geophys. Res.* 67:4427–40
- Bailey H, Senior B, Simmons D, Rusin J, Picken G, Thompson PM. 2010. Assessing underwater noise levels during pile-driving at an offshore windfarm and its potential effects on marine mammals. *Mar. Pollut. Bull.* 60:888–97
- Bannister RW. 1986. Deep sound channel noise from high-latitude winds. *J. Acoust. Soc. Am.* 79:41–48
- Barnes C, Tunnicliffe V. 2008. Building the world's first multi-node cabled ocean observatories (NEPTUNE Canada and VENUS, Canada): science, realities, challenges and opportunities. In *OCEANS 2008: MTS/IEEE Kobe Techno-Ocean*, Kobe, Japan, April 8–11. Piscataway, NJ: Inst. Electr. Electron. Eng. <http://ieeexplore.ieee.org/xpl/articleDetails.jsp?arnumber=4531076>
- Baumgartner MF, Van Parijs SM, Wenzel FW, Tremblay CJ, Esch HC, Warde AM. 2008. Low frequency vocalizations attributed to sei whales (*Balaenoptera borealis*). *J. Acoust. Soc. Am.* 124:1339–49
- Blackman DK, de Groot-Hedlin C, Harben P, Sauter A, Orcutt JA. 2004. Testing low/very low frequency acoustic sources for basin-wide propagation in the Indian Ocean. *J. Acoust. Soc. Am.* 116:2057–66
- Boyd IL, Frisk G, Urban E, Tyack P, Ausubel J, et al. 2011. An international quiet ocean experiment. *Oceanography* 24(2):174–81
- Breitz ND, Medwin H. 1989. Instrumentation for in-situ acoustical measurements of bubble spectra under breaking waves. *J. Acoust. Soc. Am.* 86:739–43
- Brekhovskikh LM, Lysanov YP. 2003. *Fundamentals of Ocean Acoustics*. New York: Springer-Verlag. 3rd ed.
- Burgess AS, Kewley DJ. 1983. Wind-generated surface noise source levels in deep water east of Australia. *J. Acoust. Soc. Am.* 73:201–10
- Butler R, Chave AD, Duennebieer FK, Yoerger DR, Petitt R, et al. 2000. Hawaii-2 observatory pioneers opportunities for remote instrumentation in ocean studies. *Eos Trans. AGU* 81:157–63
- Carey WM, Browning D. 1988. Low frequency ocean ambient noise: measurements and theory. In *Sea Surface Sound: Natural Mechanisms of Surface Generated Noise in the Ocean*, ed. BR Kerman, pp. 361–76. Dordrecht: Kluwer
- Carey WM, Evans RB. 2011. *Ocean Ambient Noise: Measurement and Theory*. New York: Springer
- Carlson RL, Schafernaar CH, Moore RP. 1984. Causes of compressional-wave anisotropy in carbonate-bearing, deep-sea sediments. *Geophysics* 49:525–32
- Castellote M, Clark CW, Lammers MO. 2011. Fin whale (*Balaenoptera physalus*) population identity in the western Mediterranean Sea. *Mar. Mamm. Sci.* 28:325–44
- Castellote M, Clark CW, Lammers MO. 2012. Acoustic and behavioural changes by fin whales (*Balaenoptera physalus*) in response to shipping and airgun noise. *Biol. Conserv.* 147:115–22
- Cato DH. 1976. Ambient sea noise in waters near Australia. *J. Acoust. Soc. Am.* 60:320–28
- Cato DH. 1991. Theoretical and measured underwater noises from surface wave orbital motion. *J. Acoust. Soc. Am.* 89:1096–112
- Chapman NR, Price A. 2011. Low frequency deep ocean ambient noise trend in the Northeast Pacific Ocean. *J. Acoust. Soc. Am.* 129:EL161–65
- Chapp E, Bohnenstiehl DR, Tolstoy M. 2005. Sound-channel observations of ice-generated tremor in the Indian Ocean. *Geochem. Geophys. Geosyst.* 6:Q06003
- Charif R, Mellinger D, Dunsmore K, Fristrup K, Clark C. 2002. Estimated source levels of fin whale (*Balaenoptera physalus*) vocalizations: adjustments for surface interference. *Mar. Mamm. Sci.* 18:81–98
- Clark C, Ellison W, Southall B, Hatch L, Van Parijs SM, et al. 2009. Acoustic masking in marine ecosystems: intuitions, analysis, and implication. *Mar. Ecol. Prog. Ser.* 395:201–22
- Clay CS, Medwin H. 1977. *Acoustical Oceanography: Principles and Applications*. New York: Wiley & Sons
- Collins MD, Coury RA, Siegmann WL. 1995. Beach acoustics. *J. Acoust. Soc. Am.* 97:2767–70
- Colton T. 2010. *Growth of the world fleet*. <http://www.shipbuildinghistory.com/today/statistics/wldftgrowth.htm>

- Cowen JP, Baker ET, Embley RW. 2004. Detection of and response to mid-ocean ridge magmatic events: implications for the subsurface biosphere. In *The Subsurface Biosphere at Mid-Ocean Ridges*, ed. WSD Wilcock, EF DeLong, DS Kelley, JS Baross, SC Cary, pp. 227–43. Washington, DC: Am. Geophys. Union
- Croll DA, Clark CW, Acevedo A, Tershy B, Flores S, et al. 2002. Only male fin whales sing loud songs. *Nature* 417:809
- Cummings W, Thompson P. 1971. Underwater sounds from the blue whale, *Balaenoptera musculus*. *J. Acoust. Soc. Am.* 50:1193–98
- Cummings WC, Thompson PO, Ha SJ. 1986. Sounds from Bryde, *Balaenoptera edeni*, and finback, *B. physalus*, whales in the Gulf of California. *Fish. Bull.* 84:359–70
- Cuyvers L. 1984. *Ocean Uses and Their Regulation*. New York: Wiley & Sons
- Deane G. 1997. Sound generation and air entrainment by breaking waves in the surf zone. *J. Acoust. Soc. Am.* 102:2671–99
- de Groot-Hedlin CD, Orcutt JA. 2001a. Excitation of T-phases by seafloor scattering. *J. Acoust. Soc. Am.* 109:1944–54
- de Groot-Hedlin CD, Orcutt JA. 2001b. T-phase observations in northern California: acoustic to seismic coupling at a weakly elastic boundary. *Pure Appl. Geophys.* 158:513–30
- Delaney JR, Kelley DS. 2014. Next-generation science in the ocean basins: expanding the oceanographer’s tool-box utilizing submarine electro-optical sensor networks. In *Seafloor Observatories: A New Vision of the Earth from the Abyss*, ed. P Favali, A de Santis, L Beranzoli. Chichester, UK: Springer Praxis. In press
- Delaney JR, Kelley DS, Lilley MD, Butterfield DA, Baross JA, et al. 1998. The quantum event of oceanic crustal accretion: impacts of diking at mid-ocean ridges. *Science* 281:222–30
- Delarue J, Todd SK, Van Parijs SM, Di Iorio L. 2009. Geographic variation in Northwest Atlantic fin whale (*Balaenoptera physalus*) song: implications for stock structure assessment. *J. Acoust. Soc. Am.* 125:1774–82
- Di Iorio L, Clark CW. 2010. Exposure to seismic survey alters blue whale acoustic communication. *Biol. Lett.* 6:51–54
- Dorman LD, Schreiner AE, Bibee LD, Hildebrand JA. 1993. Deep water seafloor array observations of seismo-acoustic noise in the eastern Pacific and comparisons with wind and swell. In *Natural Physical Sources of Underwater Sound: Sea Surface Sound (2)*, ed. BR Kerman, pp. 165–74. Norwell, MA: Kluwer
- Duennebieer FK, Lukas R, Nosal E, Aucan J, Weller R. 2012. Wind, waves and acoustic background levels at Station ALOHA. *J. Geophys. Res.* 117:C03017
- Dunn RA, Hernandez O. 2009. Tracking blue whales in the eastern tropical Pacific with an ocean-bottom seismometer and hydrophone array. *J. Acoust. Soc. Am.* 126:1084–94
- Dushaw BD, Howe BM, Mercer JA, Spindel RC, Baggeroer AB, et al. 1999. Multimegameter-range acoustic data obtained by bottom-mounted hydrophone arrays for measurement of ocean temperature. *IEEE J. Ocean. Eng.* 24:202–14
- Dyer I. 1988. Arctic ambient noise: ice source mechanics. *J. Acoust. Soc. Am.* 84:1941–42
- Dziak RP, Bohnenstiehl DR, Smith DK. 2012. Hydroacoustic monitoring of oceanic spreading centers. *Oceanography* 25(1):116–27
- Dziak RP, Hammond SR, Fox CG. 2011. A 20-year hydroacoustic series of seismic and volcanic events in the northeast Pacific Ocean. *Oceanography* 24(3):280–93
- Emery L, Bradley M, Hall T. 2001. *Database Description (DBD) for the Historical Temporal Shipping Database Variable Resolution (HITS), Version 4.0*. PSI Tech. Rep. TRS-301, Plan. Syst. Inc., Slidell, LA
- Erbe C. 2009. Underwater noise from pile driving in Moreton Bay, Qld. *Acoust. Aust.* 37:87–92
- Etter P. 2003. *Underwater Acoustic Modeling and Simulation*. London: Spon. 3rd ed.
- Ewing J, Carter JA, Sutton GH, Barstow N. 1992. Shallow-water sediment properties derived from high-frequency shear and interface waves. *J. Geophys. Res.* 97:4739–62
- Farmer DM, Vagle S, Booth AD. 1998. A free-flooding acoustical resonator for measurement of bubble size distributions. *J. Atmos. Ocean. Technol.* 15:1132–46
- Farmer DM, Xie Y. 1989. The sound generated by propagating cracks in sea ice. *J. Acoust. Soc. Am.* 85:1489–500
- Farrell WE, Munk WH. 2013. Surface gravity-waves and their acoustic signatures, 1–30 Hz, on the mid-Pacific sea floor. *J. Acoust. Soc. Am.* 134:3134–43

- Flatté SM, Dashen R, Munk WH, Watson KM, Zachariasen F. 1979. *Sound Transmission Through a Fluctuating Ocean*. Cambridge, UK: Cambridge Univ. Press
- Fox CG, Dziak RP, Matsumoto H, Schreiner AE. 1994. Potential for monitoring low-level seismicity on the Juan de Fuca Ridge using military hydrophone arrays. *Mar. Technol. Soc. J.* 27(4):22–30
- Fox CG, Hammond SR. 1994. The VENTS Program T-phase project and NOAA's role in ocean environmental research. *Mar. Technol. Soc. J.* 27(4):70–74
- Fox CG, Radford WE, Dziak RP, Lau T-K, Matsumoto H, Schreiner AE. 1995. Acoustic detection of a seafloor spreading episode on the Juan de Fuca Ridge using military hydrophone arrays. *Geophys. Res. Lett.* 22:131–34
- Frankel AS, Clark CW. 1998. Results of low-frequency playback of M-sequence noise to humpback whales, *Megaptera novaeangliae*, in Hawai'i. *Can. J. Zool.* 76:521–35
- Frankel AS, Clark CW. 2000. Behavioral responses of humpback whales (*Megaptera novaeangliae*) to full-scale ATOC signals. *J. Acoust. Soc. Am.* 108:1930–37
- Frisk GV. 2012. Noiseconomics: the relationship between ambient noise levels in the sea and global economic trends. *Sci. Rep.* 2:437
- Gavrilov AN, McCauley RD, Gedamke J. 2012. Steady inter and intra-annual decrease in the vocalization frequency of Antarctic blue whales. *J. Acoust. Soc. Am.* 131:4476–80
- Gavrilov I, Li B. 2008. Long-term variations of ice breaking noise in Antarctica. *J. Acoust. Soc. Am.* 123:2989 (Abstr.)
- Godin O. 1998. A note on differential equations of coupled-mode propagation in fluids. *J. Acoust. Soc. Am.* 103:159–68
- Hanson J, Le Bras R, Dysart P, Brumbaugh D, Gault A, Guern J. 2001. Operational processing of hydroacoustics at the prototype international data center. *Pure Appl. Geophys.* 158:425–56
- Hatch LT, Clark CW, Van Parijs SM, Frankel AS, Ponirakis DW. 2012. Quantifying loss of acoustic communication space for right whales in and around a U.S. national marine sanctuary. *Conserv. Biol.* 26:983–94
- Haxel JH, Dziak RP, Matsumoto H. 2013. Observations of shallow water marine ambient sound: the low frequency underwater soundscape of the central Oregon coast. *J. Acoust. Soc. Am.* 133:2586–96
- Holland CW. 2010. Propagation in a waveguide with range-dependent seabed properties. *J. Acoust. Soc. Am.* 128:2596–609
- Ikelle L, Amundsen L. 2005. *Introduction to Petroleum Seismology*. Tulsa, OK: Soc. Explor. Geophys
- Int. Marit. Organ. 2011. *International shipping facts and figures—information resources on trade, safety, security, environment*. Rep., Int. Marit. Organ., London
- Johnson BD, Cooke RC. 1979. Bubble populations and spectra in coastal water: a photographic approach. *J. Geophys Res.* 84:3761–66
- Johnson RH, Northrop J, Eppley R. 1963. Sources of Pacific T-phases. *J. Geophys. Res.* 68:4251–60
- Kasahara J, Iwase R, Nakatsuka T, Nagaya Y, Shirasaki Y, et al. 2006. An experimental multi-disciplinary observatory (VENUS) at the Ryukyu trench using the Guam-Okinawa geophysical submarine cable. *Ann. Geophys.* 49:595–606
- Kawaguchi K, Kaneda Y, Araki E. 2008. The DONET: a real-time seafloor research infrastructure for the precise earthquake and tsunami monitoring. In *OCEANS 2008: MTS/IEEE Kobe Techno-Ocean*, Kobe, Japan, April 8–11. Piscataway, NJ: Inst. Electr. Electron. Eng. <http://ieeexplore.ieee.org/xpl/articleDetails.jsp?arnumber=4530918>
- Koch RA, Penland C, Vidmar PJ, Hawker KE. 1983. On the calculation of normal mode group-velocity and attenuation. *J. Acoust. Soc. Am.* 73:820–25
- Koesoemadinata AP, McMechan GA. 2004. Effects of diagenetic processes on seismic velocity anisotropy in near-surface sandstone and carbonate rocks. *J. Appl. Geophys.* 56:165–76
- Leigh CV, Eller AI. 2008. *Dynamic ambient noise model comparison with Point Sur, California, in situ data*. Tech. Memo. APL-UW TM 2-06, Appl. Phys. Lab., Univ. Wash., Seattle
- Lewis JK, Denner WW. 1988. Arctic ambient noise in the Beaufort Sea: seasonal relationships to sea ice kinematics. *J. Acoust. Soc. Am.* 83:549–65
- Longuet-Higgins MS. 1950. A theory for the generation of microseisms. *Philos. Trans. R. Soc. Lond. A* 24:1–35
- Martin BE, Thomson CJ. 1997. Modelling surface waves in anisotropic structures II: examples. *Phys. Earth Planet. Inter.* 103:253–97

- McCreery CS, Duennebier FK, Sutton GH. 1993. Correlation of deep ocean noise (0.4–30 Hz) with wind, and the Holu spectrum—a worldwide constant. *J. Acoust. Soc. Am.* 93:2639–48
- McDonald MA, Hildebrand JA, Mesnick S. 2009. Worldwide decline in tonal frequencies of blue whale songs. *Endanger. Species Res.* 9:13–21
- McDonald MA, Hildebrand JA, Webb SC. 1995. Blue and fin whales observed on a seafloor array in the Northeast Pacific. *J. Acoust. Soc. Am.* 98:712–21
- McDonald MA, Hildebrand JA, Wiggins SM. 2006. Increases in deep ocean ambient noise in the Northeast Pacific west of San Nicolas Island, California. *J. Acoust. Soc. Am.* 120:711–18
- McGuire JJ, Collins JA, Gouedard P, Roland E, Lizarralde D, et al. 2012. Capturing the end of a seismic cycle on the Gofar Transform Fault. *Nat. Geosci.* 5:336–41
- McKenna MF, Katz SL, Wiggins SM, Ross D, Hildebrand JA. 2012a. A quieting ocean: unintended consequence of a fluctuating economy. *J. Acoust. Soc. Am.* 132:169–75
- McKenna MF, Ross D, Wiggins SM, Hildebrand JA. 2012b. Underwater radiated noise from modern commercial ships. *J. Acoust. Soc. Am.* 131:92–103
- Mikhalevsky PN, Gavrilov AN. 2001. Acoustic thermometry in the Arctic Ocean. *Polar Res.* 20:185–92
- Mikhalevsky PN, Gavrilov AN, Baggeroer AB. 1999. The Transarctic Acoustic Propagation Experiment and climate monitoring in the Arctic. *IEEE J. Ocean. Eng.* 24:183–201
- Minnaert M. 1933. On musical air bubbles and the sounds of running water. *Philos. Mag.* 16:235–48
- Mobley JR. 2005. Assessing responses of humpback whales to North Pacific Acoustic Laboratory (NPAL) transmissions: results of 2001–2003 aerial surveys north of Kauai. *J. Acoust. Soc. Am.* 117:1666–73
- Munk WH, Forbes AMG. 1989. Global ocean warming: an acoustic measure? *J. Phys. Oceanogr.* 19:1765–78
- Munk WH, Worcester P, Wunsch C. 1995. The forward problem: range-independent. In *Ocean Acoustic Tomography*, pp. 30–114. Cambridge, UK: Cambridge Univ. Press
- Natl. Ocean. Atmos. Adm. 2012. *Mapping cetaceans and sound: modern tools for ocean management*. Symp. Final Rep., Natl. Ocean. Atmos. Adm., Washington, DC. http://cetsound.noaa.gov/pdf/CetSound_Symposium_Report_Final.pdf
- Nieukirk SL, Mellinger DK, Moore SE, Klinck K, Dziak RP, Goslin J. 2012. Sounds from airguns and fin whales recorded in the mid-Atlantic Ocean, 1999–2009. *J. Acoust. Soc. Am.* 131:1102–12
- Nieukirk SL, Stafford KM, Mellinger DK, Dziak RP, Fox CG. 2004. Low-frequency whale and seismic airgun sounds recorded in the mid-Atlantic Ocean. *J. Acoust. Soc. Am.* 115:1832–43
- Nishimura CE, Conlon DM. 1994. IUSS dual use: monitoring whales and earthquakes using SOSUS. *Mar. Technol. Soc. J.* 27(4):13–21
- Nolet G, Dorman LM. 1996. Waveform analysis of Scholte modes in ocean sediment layers. *Geophys. J. Int.* 125:385–96
- Offshore*. 2012. Worldwide seismic vessel survey. *Offshore* 72(3):36–41
- Okal A. 2008. The generation of *T* waves by earthquakes. *Adv. Geophys.* 49:1–65
- Oleson EM, Barlow J, Gordon J, Rankin S, Hildebrand JA. 2003. Low frequency calls of Bryde’s whales. *Mar. Mamm. Sci.* 19:407–19
- Oleson EM, Calambokidis J, Burgess WC, McDonald MA, LeDuc CA, Hildebrand JA. 2007. Behavioral context of call production by eastern North Pacific blue whales. *Mar. Ecol. Prog. Ser.* 330:269–84
- Park J. 1996. Surface waves in layered anisotropic structures. *Geophys. J. Int.* 126:173–83
- Park M, Odom RI, Soukup DJ. 2001. Modal scattering: a key to understanding oceanic *T*-waves. *Geophys. Res. Lett.* 28:3401–4
- Payne RR, Webb DD. 1971. Orientation by means of long range acoustic signaling in baleen whales. *Ann. N. Y. Acad. Sci.* 188:110–41
- Porter MB, Henderson LJ. 2013. Global ocean soundscapes. *Proc. Meet. Acoust.* 19:010050
- Priede IJ, Solan M, eds. 2002. *ESONET: European Seafloor Observatory Network*. Rep. EVK3-EVK3-CT-2002-80008, Univ. Aberdeen, Aberdeen, UK
- Rankin S, Barlow J. 2007. Vocalizations of the sei whale *Balaenoptera borealis* off the Hawaiian Islands. *Bioacoustics* 16:137–45
- Rebull OG, Cusi JD, Fernandez MR, Muset JG. 2006. Tracking fin whale calls offshore the Galacia Margin, NE Atlantic Ocean. *J. Acoust. Soc. Am.* 120:2077–85

- Reinhal PG, Dahl PH. 2011. Underwater Mach wave radiation from impact pile driving: theory and observation. *J. Acoust. Soc. Am.* 130:1209–16
- Rolland RM, Parks SE, Hunt KE, Castellote M, Corkeron PJ, et al. 2012. Evidence that ship noise increases stress in right whales. *Proc. R. Soc. B* 279:2363–68
- Ross DG. 1976. *Mechanics of Underwater Noise*. New York: Pergamon
- Ross DG. 1993. On ocean underwater ambient noise. *Acoust. Bull.* 18:5–8
- Roth E, Hildebrand J, Wiggins S, Ross D. 2012. Underwater ambient noise on the Chukchi Sea continental slope from 2006–2009. *J. Acoust. Soc. Am.* 131:104–10
- Scholte JG. 1947. Range of existence of Rayleigh and Stoneley waves. *Geophys. J. Int.* (Suppl. S5) 5:120–26
- Shearer PM. 2009. *Introduction to Seismology*. New York: Cambridge Univ. Press. 2nd ed.
- Sheriff RE, Geldart LP. 1995. *Exploration Seismology*. New York: Cambridge Univ. Press. 2nd ed.
- Simon M, Stafford KM, Beedholm K, Lee CM, Madsen PT. 2010. Singing behavior of fin whales in the Davis Strait with implications for mating, migration and foraging. *J. Acoust. Soc. Am.* 128:3200–10
- Širović A, Hildebrand JA, Wiggins SM. 2007. Blue and fin whale call source levels and propagation range in the Southern Ocean. *J. Acoust. Soc. Am.* 122:1208–15
- Širović A, Hildebrand JA, Wiggins SM, Thiele D. 2009. Blue and fin whale acoustic presence around Antarctica during 2003 and 2004. *Mar. Mamm. Sci.* 25:125–36
- Smith KB, Brown MG, Tappert FD. 1992. Ray chaos in underwater acoustics. *J. Acoust. Soc. Am.* 91:1939–49
- Soukup DJ, Odom RI, Park J. 2013. A modal investigation of elastic anisotropy in shallow water environments: a study of anisotropy beyond VTI. *J. Acoust. Soc. Am.* 134:185–207
- Soule DC, Wilcock WSD. 2012. Fin whale tracks recorded by a seismic network on the Juan de Fuca Ridge, Northeast Pacific Ocean. *J. Acoust. Soc. Am.* 133:1751–61
- Stafford KM, Chapp E, Bohnenstiel DR, Tolstoy M. 2011. Seasonal detection of three types of “pygmy” blue whale calls in the Indian Ocean. *Mar. Mamm. Sci.* 27:828–40
- Stafford KM, Nieuwirk SL, Fox CG. 2001. Geographic and seasonal variation of blue whale calls in the North Pacific. *J. Cetacean Res. Manag.* 3:65–76
- Stoll RD, Bryan GM, Bautista EO. 1994. Measuring lateral variability of sediment geoacoustic properties. *J. Acoust. Soc. Am.* 96:427–38
- Stone RG, Mintzer D. 1962. Experimental study of high-frequency sound propagation in a randomly inhomogeneous medium. *J. Acoust. Soc. Am.* 34:735–36
- Talandier J, Hyvernaud O, Okal EA. 2002. Long-range detection of hydroacoustic signals from large icebergs in the Ross Sea, Antarctica. *Earth Planet. Sci. Lett.* 203:519–34
- Talandier J, Hyvernaud O, Reymond D, Okal EA. 2006. Hydroacoustic signals generated by parked and drifting icebergs in the Southern Indian and Pacific Oceans. *Geophys. J. Int.* 165:817–34
- Tanner G, Sondergaard N. 2007. Wave chaos in acoustics and elasticity. *J. Phys. A* 40:R443–509
- Thode AM, D’Spain GL, Kuperman WA. 2000. Matched-field processing, geoacoustic inversion, and source signature recovery of blue whale vocalizations. *J. Acoust. Soc. Am.* 107:1286–300
- Tolstoy M, Cowen JP, Baker ET, Fornari DJ, Fubin KH, et al. 2006. A seafloor spreading event captured by seismometers. *Science* 314:1920–22
- Tolstoy M, Diebold J, Doermann L, Nooner S, Webb SC. 2009. Broadband calibration of the R/V *Marcus G. Langseth* four-string seismic sources. *Geochem. Geophys. Geosyst.* 10:Q08011
- Tougaard J, Henriksen OD, Miller LA. 2009. Underwater noise from three types of offshore wind turbines: estimation of impact zones for harbor porpoises and harbor seals. *J. Acoust. Soc. Am.* 25:3766–73
- Urick RJ. 1983. *Principles of Underwater Sound*. New York: McGraw-Hill. 3rd ed.
- Valcke SLA, Casey M, Lloyd GE, Kendall J-M, Fisher QJ. 2006. Lattice preferred orientation and seismic anisotropy in sedimentary rocks. *Geophys. J. Int.* 166:652–66
- Virovlyansky AL. 2008. Ray chaos in underwater acoustic waveguides. *Int. J. Bifurc. Chaos* 18:2693–700
- Walbridge S. 2013. *Assessing ship movements using volunteered geographic information*. PhD thesis, Univ. Calif., Santa Barbara
- Wales SC, Heitmeyer RM. 2002. An ensemble source spectra model for merchant ship-radiated noise. *J. Acoust. Soc. Am.* 111:1211–31
- Walker DA. 1981. High-frequency Pn, Sn velocities: some comparisons for the western, central, and south Pacific. *Geophys. Res. Lett.* 8:207–9

- Walker DA, McCreery CS, Sutton GH. 1983. Spectral characteristics of high-frequency P_N, S_N phases in the western Pacific. *J. Geophys. Res.* 88:4289–98
- Watkins WA. 1981. Activities and underwater sounds of fin whales [*Balaenoptera physalus*]. *Sci. Rep. Whales Res. Inst.* 33:83–117
- Watkins WA, Tyack P, Moore K, Bird J. 1987. The 20-Hz signals of finback whales (*Balaenoptera physalus*). *J. Acoust. Soc. Am.* 82:1901–12
- Webb SC. 1998. Broadband seismology and noise under the ocean. *Rev. Geophys.* 36:105–42
- Weekly RT, Wilcock WSD, Hooft EEE, Toomey DR, McGill PR, Stakes DS. 2013. Termination of a decadal-scale ridge-spreading event observed using a seafloor seismic network on the Endeavour segment, Juan de Fuca Ridge. *Geochem. Geophys. Geosyst.* In press
- Weirathmueller MJ, Wilcock WSD, Soule DC. 2013. Source levels of fin whale 20 Hz pulses measured in the Northeast Pacific Ocean. *J. Acoust. Soc. Am.* 133:741–49
- Wenz GM. 1962. Acoustic ambient noise in the ocean: spectra and sources. *J. Acoust. Soc. Am.* 34:1936–56
- Wilcock WSD, Webb SC, Bjarnason IT. 1999. The effect of local wind on seismic noise near 1 Hz at the MELT site and in Iceland. *Bull. Seismol. Soc. Am.* 89:1543–57
- Worcester PF, Spindel RC. 2005. North Pacific Acoustic Laboratory. *J. Acoust. Soc. Am.* 117:1499–510
- Yoon SW, Crum LA, Prosperetti A, Lu NQ. 1991. An investigation of the collective oscillation of a bubble cloud. *J. Acoust. Soc. Am.* 89:700–6
- Zampolli M, Nijhof MJJ, de Jong CAF, Ainslie MA, Jansen EHW, Quesson BAJ. 2012. Validation of finite element computations for the quantitative prediction of underwater noise from impact pile driving. *J. Acoust. Soc. Am.* 133:72–81



Contents

Shedding Light on the Sea: André Morel's Legacy to Optical Oceanography <i>David Antoine, Marcel Babin, Jean-François Berthon, Annick Bricaud, Bernard Gentili, Hubert Loisel, Stéphane Maritorena, and Dariusz Stramski</i>	1
Benthic Exchange and Biogeochemical Cycling in Permeable Sediments <i>Markus Huettel, Peter Berg, and Joel E. Kostka</i>	23
Contemporary Sediment-Transport Processes in Submarine Canyons <i>Pere Puig, Albert Palanques, and Jacobo Martín</i>	53
El Niño Physics and El Niño Predictability <i>Allan J. Clarke</i>	79
Turbulence in the Upper-Ocean Mixed Layer <i>Eric A. D'Asaro</i>	101
Sounds in the Ocean at 1–100 Hz <i>William S.D. Wilcock, Kathleen M. Stafford, Rex K. Andrew, and Robert I. Odom</i> ..	117
The Physics of Broadcast Spawning in Benthic Invertebrates <i>John P. Crimaldi and Richard K. Zimmer</i>	141
Resurrecting the Ecological Underpinnings of Ocean Plankton Blooms <i>Michael J. Behrenfeld and Emmanuel S. Boss</i>	167
Carbon Cycling and Storage in Mangrove Forests <i>Daniel M. Alongi</i>	195
Ocean Acidification in the Coastal Zone from an Organism's Perspective: Multiple System Parameters, Frequency Domains, and Habitats <i>George G. Waldbusser and Joseph E. Salisbury</i>	221
Climate Change Influences on Marine Infectious Diseases: Implications for Management and Society <i>Colleen A. Burge, C. Mark Eakin, Carolyn S. Friedman, Brett Froelich, Paul K. Hershberger, Eileen E. Hofmann, Laura E. Petes, Katherine C. Prager, Ernesto Weil, Bette L. Willis, Susan E. Ford, and C. Drew Harvell</i>	249

Microbially Mediated Transformations of Phosphorus in the Sea: New Views of an Old Cycle <i>David M. Karl</i>	279
The Role of B Vitamins in Marine Biogeochemistry <i>Sergio A. Sañudo-Wilhelmy, Laura Gómez-Consarnau, Christopher Suffridge, and Eric A. Webb</i>	339
Hide and Seek in the Open Sea: Pelagic Camouflage and Visual Countermeasures <i>Sönke Johnsen</i>	369
Antagonistic Coevolution of Marine Planktonic Viruses and Their Hosts <i>Jennifer B.H. Martiny, Lasse Riemann, Marcia F. Marston, and Mathias Middelboe</i>	393
Tropical Marginal Seas: Priority Regions for Managing Marine Biodiversity and Ecosystem Function <i>A. David McKinnon, Alan Williams, Jock Young, Daniela Ceccarelli, Piers Dunstan, Robert J.W. Brewin, Reg Watson, Richard Brinkman, Mike Cappo, Samantha Duggan, Russell Kelley, Ken Ridgway, Dbugal Lindsay, Daniel Gledhill, Trevor Hutton, and Anthony J. Richardson</i>	415
Sea Ice Ecosystems <i>Kevin R. Arrigo</i>	439
The Oceanography and Ecology of the Ross Sea <i>Walker O. Smith Jr., David G. Ainley, Kevin R. Arrigo, and Michael S. Dinniman</i>	469

Errata

An online log of corrections to *Annual Review of Marine Science* articles may be found at <http://www.annualreviews.org/errata/marine>